Heliyon 7 (2021) e08459

Contents lists available at ScienceDirect

Heliyon

journal homepage: www.cell.com/heliyon

Research article

Green synthesis of silver nanoparticles using *Hagenia abyssinica (Bruce) J.F. Gmel* plant leaf extract and their antibacterial and anti-oxidant activities

Walelign Wubet Melkamu *, Legesse Terefe Bitew

Department of Chemistry, College of Natural & Computational Sciences, University of Gondar, Ethiopia

ARTICLE INFO

Keywords:
Anti-bacterial activity
Anti-oxidant activity
Green synthesis
Hagenia abyssinica
Silver nanoparticles

ABSTRACT

Green synthesis of silver nanoparticles (AgNPs) was achieved by bio-reduction of silver nitrate using *Hagenia Abyssinica* plant leaf extract (HAPLE). The AgNPs formation was confirmed by Ultraviolet-Visible (UV-Vis) spectrophotometer. The synthesized AgNPs in solution have shown maximum absorption at 430 nm. The different parameters like temperature, pH, time, silver nitrate concentration and volume of leaf extract were optimized spectrophotometrically. The Fourier-Transform Infrared (FTIR) Spectroscopy was used to confirm the existence of various functional groups responsible for reducing and stabilizing during the biosynthesis process. The X-Ray Diffraction (XRD) analysis confirmed the structure, crystal size and nature of the AgNPs. The synthesized AgNPs showed antimicrobial (gram-negative bacteria (*klebsiella pneumoniae* and *salmonella typhimurium*) and gram-positive bacteria (*Streptococcus pneumoniae*)) and antioxidant (2,2-diphenyl-1-picryl-hydrazyl (DPPH) radical scavenging method) activities. The developed method for the AgNPs synthesis using HAPLE is an eco-friendly and convenient method. In near future, the synthesized AgNPs could be used in the fields of water treatment, biomedicine, biosensor and nanotechnology.

1. Introduction

The scientific community showed a great interest in nanomaterials due to their unique properties and versatile applications in biomedical fields and for environmental remediation [1]. Biomedicine, drug delivery, bio-imaging, bio-labeling, photovoltaics, photocatalysis, solar cells, and data storage are among the promising fields of nanomaterials [2]. AgNPs have been paid special attention due to the reduction in antibiotics efficiency and development against highly resistant microbes [3]. Several synthesis routes have been proposed to synthesize AgNPs. AgNPs have been prepared via physical, chemical and biological synthesis routes. The chemicals used for the synthesis and stabilization of AgNPs are toxic, expensive, and often lead to non-eco-friendly by-products. Recently, biological methods provide a better alternative platform for the synthesis of AgNPs [4]. The green synthesis approach is the most advantages over the chemical and physical method as it is cost-effective, eco-friendly, and easy to scale up for large-scale synthesis without applying energy, high pressure, temperature, and toxic chemicals [5].

Nowadays, there is a growing interest to use economical and environmentally friendly and green synthesis routes that use non-toxic chemicals in the synthesis protocol of AgNPs. Alternative green synthesis of AgNPs using several microorganisms, plants, and algae is natural, biocompatible, and environmentally safe methods. The use of plant materials can be more beneficial for AgNPs synthesis than bacterial and chemical methods because of no threat of bacterial and dangerous chemical contamination and less energy utilization with wider implications and easiness [6]. Recently, the biosynthesis of AgNPs using plant extract and microbes as reducing agents and their antimicrobial activity is widely investigated. The biomolecules such as flavonoids, ketones, aldehydes, tannins, carboxylic acids, phenolic, and the protein of the plant extracts are responsible for the production of AgNPs by reducing Ag^{+} to Ag^{0} [7]. The biosynthesized AgNPS exhibit different sizes, shapes, and morphology. All these properties are strongly influenced under different experimental conditions such as temperature, pH, the kinetics of interaction between metal salts and reducing agents, nature, and adsorption of capping agents. The properties of AgNPs depend on their size, shape, and morphology [4, 8]. As a result, designing a process that controls the size, shape, stability, and physicochemical properties is currently the most important part of research into nanoparticle synthesis [9].

Although the exact mechanism of nanoparticles biosynthesis by various plant extracts is ambiguous, it has been proposed that the biomolecules in plant extract such as protein, phenol and flavonoids play a

* Corresponding author.
E-mail address: wwalelign@gmail.com (W.W. Melkamu).

https://doi.org/10.1016/j.heliyon.2021.e08459
Received 27 July 2021; Received in revised form 13 October 2021; Accepted 18 November 2021

significant role in the reduction of metals ions and capping the bio-synthesized nanoparticles [10]. According to the previous studies, the mechanism of bio-reduction can be divided into three main steps: (1) silver ion reduction and nucleation, (2) the growing step and aggregation, and (3) capping and stabilization in the terminal step. The crucial role is always played by the phytochemicals of the plant, namely, secondary metabolites such as sugars, polyphenols, proteins, phenolic acids, ketones, terpenoids, amides, etc. Moreover, in the majority of cases, a reducing agent from the plant extract plays a role as both the capping and stabilizing agents [11].

AgNPs have strong inhibitory and bacterial effects, which have been used to prevent and treat various diseases [12, 13, 14, 15, 16]. The antimicrobial mechanisms of AgNPs on multidrug-resistant bacteria remain enigmatic. Previous studies reported their observations of AgNPs against *Escherichia coli* and revealed that formation of "pits" in bacterial cell wall and accumulation of AgNPs in the cellular membrane led to an augmented permeability of the cell wall and ultimately the cell death, AgNPs were able to kill or curb *Staphylococcus aureus* or *Salmonella typhimurium*, and their antibacterial performance strongly relied on the dimension of the particles. Only very few studies reported that AgNPs had antimicrobial activity on multidrug-resistant *P. aeruginosa* [17].

In 2017, the World Health Organization (WHO) has published a list of antibiotic-resistant priority pathogens, pathogens which present a great threat to humans and to which new antibiotics are urgently needed. The list is categorized according to the urgency of need for new antibiotics as critical, high, and medium priority, in order to guide and promote research and development of new antibiotics. The majority of the WHO list is Gram-negative bacterial pathogens. Due to their distinctive structure, Gram-negative bacteria are more resistant than Gram-positive bacteria, and cause significant morbidity and mortality worldwide [18].

Biological systems are damaged by the presence of free radicals. The responsible free radicals are oxygen free radicals or generally known as reactive oxygen species (ROS) [19]. In recent years, the search for effective, non-toxic, natural compounds with antioxidative activity has been increased. The strong antioxidant property exhibited by some nanomaterials is opening exciting potential to develop new regimens with enhanced and targeted actions. For instance, gold, silver and selenium nanoparticles have been shown to possess ability to reduce oxidative stress due to their efficient redox-active radical-scavenging properties [20]. Studies have shown that apple decreases the presence of ROS generated by hydrogen peroxide exposure in lymphocytes [19].

Therefore, the present study focused on the green synthesis of AgNPs using the HAPLE and evaluating its anti-oxidant and anti-bacterial activities. *Hagenia abyssinica* (Kosso) has been used as a powerful remedy for intestinal parasites, especially against cestodes (Figure 1). This plant is commonly available in Ethiopia and each part of this tree has been used as a household remedy for the treatment of tapeworm, diarrhea and stomach-ache and is sometimes taken as an abortifacient since ancient times. In the 19th century, the species was included in most European pharmacopoeias as an effective drug against intestinal worms, which made it one of the most famous African plants at that time [21]. AgNPs using HAPLE has been synthesized for the electrochemical activities study [22] but to the best of our knowledge and literature survey, there has been no study on the anti-oxidant and anti-bacterial activities of Silver nano-particles synhesized using HAPLE. Our investigation was therefore focused on the physicochemical characterization of the bio-synthesized nanoparticles using UV-Visible spectrophotometer, XRD and FTIR. In addition, the anti-bacterial activity of the synthesized AgNPs against gram-negative bacteria *(klebsiella pneumoniae* and *salmonella typhimurium)* and gram-positive bacteria (*Streptococcus pneumoniae*) were evaluated by standard agar well diffusion method. The anti-oxidant property of the synthesized AgNPs was analyzed by the DPPH free radical scavenging assay method.

Figure 1. Image of *Hagenia abyssinica* tree along with its flowers.

2. Materials and methods

All the chemicals and reagents used in this study were of analytical grade and double distilled water was used throughout the experiment. Silver nitrate ($AgNO_3$, 99.8% was purchased from Himedia Laboratories Pvt. Ltd., Mumbai, India); Ferric chloride ($FeCl_3$, 99% from Sisco Research Laboratories (Mumbai, India); Muller-Hinton Agar (MHA, were from Merck chemical company), Chloroform ($CHCl_3$, 99.9% from Fisher Scientific UK Limited, UK), Sulphuric acid (H_2SO_4, 98%), Sodium hydroxide (NaOH, 98%), Ascorbic acid ($C_6H_8O_6$, 99.9%) were purchased from Loba Chemie Pvt. Ltd (Mumbai, India); Hydrochloric acid (HCl, 37% from Blulux laboratory reagent, India), DPPH ($C_{18}H_{12}N_5O_6$, 99% from Sigma-Aldrich Pty Ltd, Germany); and *Hagenia abyssinica (Bruce) J.F. Gmel* plant leaves.

2.1. Plant material and preparation of the extract

Following the procedure in [22] and with slight modifications, the fresh leaves of *Hagenia abyssinica* was washed with running tap water several times followed by distilled water to remove any dust particles on it. Then it was allowed to dry under shadow room temperature for 20 days to remove moisture contents from the leaves. The dried leaf was powdered using an electrical grinder to get a fine powder of the sample. The extraction was carried out by taking 50 g of plant powdered leaves in a 500 mL conical flask containing 450 mL of distilled water. It was covered with aluminum foil, to prevent the effect of light on the solution. Then the mixture was Shaked using mechanical shaker for 30 min and allowed to warm at 65 °C for 1 h on a hot-plate with magnetic stirrer, then it was allowed to cool down at room temperature. Then the prepared solution was filtered by Whatman No.1 filter paper to get the clear extract solution. The filtrate was stored at 4 °C for future experiments.

2.2. Phytochemical screening of phenols, alkaloids, flavonoids, anthraquinones, terpenoids and steroids, tannins and saponins

The aqueous leaf extracts was subjected to preliminary phytochemical screening following standard methods [23, 24, 25, 26]. The presence or absences of phytochemicals in the plant leaf extract were tested. The details of the methods used for the qualitative phytochemical screening of HAPLE.and the results on phytochemical screening test are shown in Tables 1 and 2 respectively.

Table 1. Qualitative phytochemical screening of HAPLE.

Phytochemicals	Reagent/Test	Reference
Test for phenols	**Ferric chloride test:** Two milliliters of 5% solution of $FeCl_3$ was added to 1 mL plant leaf extracts. A black colour of the reaction mixture was developed which confirms the presence of phenol.	[23]
Test for Alkaloids	**Mayer's reagent test:** 3 mL of plant leaf extract was added to 3 mL of 1% HCl solution and it was heated for 20 min on a water bath. The resulted reaction mixture was cooled at room temperature and used to perform Mayer's test. To the cooled reaction mixture in a test tube, 1 mL of Mayer's reagent was added drop by drop. The formation of a greenish colored cream precipitate indicated for the presence of alkaloids.	[25]
Test for Flavonoids	**Alkaline reagent test:** Three milliliters of plant leaf extract were treated with 1 mL of 10% NaOH solution. The formation of an intense yellow colour was indicated and it confirms the presence of flavonoids.	[24]
Test for anthraquinones	**Bontrager's test:** To 0.2 mL of plant leaf extract, 5 mL of chloroform and 5 mL of ammonia solution was added. The presence of bright pink colour in the aqueous layer indicated the presence of anthraquinones.	[26]
Test for terpenoids and steroids	**Salkowski test:** Five milliliters of plant leaf extract solution were mixed in 2 mL of chloroform, and 3 mL of conc. sulphuric acid to form a layer. A reddish-brown coloration of the interface was formed to indicate the presence of terpenoids. Red colour at the lower surface indicates presence of steroid	[24]
Test for tannins	**a) Ferric chloride test:** To 0.5 mL plant leaf extract solution, 1 mL distilled water and 2 drops of ferric chloride solution was added to it and blue-black coloration was observed which indicates the presence of tannins. **b) Lead acetate test:** 10% lead acetate solution was added to 0.5 mL of plant leaf extract solution and white precipitation was observed which confirms for the presence of tannins	[26]
Test for saponins	**Frothing test:** 0.2 mL of the plant leaf extracts was shaked with 5 mL of distilled water and then heated to boil. Frothing shows the presence of saponin.	[23]

2.3. Synthesis of AgNPs

Following the procedure in [27, 28] and with slight modifications, the AgNPs were successfully synthesized using 1:2 volume ratio (100 mL–200 mL) of $AgNO_3$ to HAPLE as a reducing and capping agent, silver nitrate as a precursor. An optimized concentration of aqueous solution of $AgNO_3$ (4 mM) was prepared in 250 mL amber volumetric flask and used for the synthesis of silver nanoparticles. For the reduction of Ag^+ ions, the optimized volume of HAPLE (200 mL) was mixed with optimized volume (100 mL) & concentration (4 mM) of $AgNO_3$ solution. The synthesis of silver nanoparticles was carried out at an optimal temperature and incubation time (40 °C and 90 min) in a closed incubator. A color change from colorless to brown was observed after optimized reaction conditions and this indicated the formation of silver nanoparticles. The reduction of Ag^+ was confirmed by the UV–Vis spectrum of the reaction solution. Finally, the silver nanoparticles were separated out from the mixture by high-speed centrifugation at 10,000 revolutions per minute (rpm) for 20 min. After centrifugation the synthesized AgNPs pellets were rinsed with 20 mL distilled water, freeze-dried by Lyophilizer, and stored at room temperature for further characterizations. Effects of concentration, reaction time, volume ratio, temperature, and pH on the formation of AgNPs were investigated. The study was monitored using double beam UV-Vis spectrophotometer (Agilent technologies, Cary 60 UV-Vis; USA). The experiment was carried out by optimizing the concentrations of $AgNO_3$ solution (0.5 mM, 1 mM, 2 mM, 4 mM, and 6 mM); reaction time (10 min, 30 min, 60 min, 90 min, and 120 min); volume ratio with respect to $AgNO_3$ to plant leaf extract (1:1, 1:2, 1:3, and 1:4); temperature of the reaction mixture (25 °C, 40 °C, 60 °C, and 80 °C); and effects of pH (pH 4, pH 6, pH 7, pH 8, and pH 9).

Table 2. Results on Phytochemical screening of HAPLE.

S/No	Bioactive phytochemicals	Test/Reagents	Result
1	Alkaloids	Mayer's reagent	+
2	Flavonoids	Alkaline reagent test	+
3	Saponins	Frothing test	+
4	Tannins	a) Lead acetate test	+
		b) Ferric chloride test	+
5	Terpenoids & Steroids	Salkowski test	−
6	Phenols	Ferric chloride test	+
7	Anthraquinones	Bontrager's test	+

Note: + = Present, and − = Absent.

2.4. Characterization of silver nanoparticles

The biosynthesis of AgNPs and the reduction of silver ions was analyzed for surface plasmon resonance (SPR) by using double beam UV-Vis spectrophotometer (Agilent technologies, Cary 60 UV-Vis; USA) in the wavelength range of 200–800 nm. The FTIR analysis was carried out using FTIR spectrometer (PerkinElmer spectrum LS-65-Luminescence; USA). The FTIR spectra of the synthesized AgNPs were obtained in the range of 4000–400 cm^{-1}. The FTIR spectrometer was used to determine the organic functional groups linked to the surface of silver nanoparticles responsible for the reduction, stabilizing and capping agents. The XRD analysis was also carried out to reveal the crystallographic nature of the biosynthesized AgNPs using advanced X-ray Diffractometer (Shimadzu Corporation (Japan); XRD-7000 X-ray Diffractometer) with Cu-Kα radiation of wavelength 1.5406 Å and scanning angle 2θ from 10° to 90°.

2.5. Antibacterial and antioxidant studies of silver nanoparticles

2.5.1. Antibacterial study

Following the procedure in [29] and with slight modifications, the antibacterial activities of biosynthesized AgNPs was performed. It was evaluated using agar well diffusion method. The antibacterial activity was studied using one gram-positive (*Streptococcus pneumoniae*) and two gram-negative (*Klebsiella pneumoniae* and *Salmonella typhimurium*) clinically isolated pathogenic bacteria. These bacteria were used for this study because they present a great threat to humans and to which new antibiotics are urgently needed. The World Health Organization (WHO) has published a list of antibiotic-resistant priority pathogens by 2017. The majority of the WHO list is Gram-negative bacterial pathogens [30]. The media used was Mueller-Hinton Agar (MHA) and it was prepared according to the manufacturer's instruction, where 35 g of powder media was mixed with one liter of distilled water and enclosed in a container and autoclaved at 121 °C for 15 min. The media were later dispensed into sterile Petri dishes. After the media was solidified, 100 μL of the working stock culture was spread with sterile cotton swab and wells were made in each Petri dish by a stainless steel cork borer. Then different concentration of AgNPs and the crude extract (50 μg/mL, 100 μg/mL, 150 μg/mL and 200 μg/mL) were prepared separately from 100 mg/mL stock solution. Wells were filled with the prepared solutions of AgNPs, extract solutions, Dimethylsulfoxide (DMSO) (negative control), ciprofloxacin (positive control) and kept in refrigerator for 30 min until it diffuses. The

petri dishes were incubated at 37 °C for 24 h. Finally, zone of inhibition of green synthesized AgNPs and the plant leaf crude extract with different concentrations against the pathogenic bacteria were measured in millimeter.

2.5.2. Antioxidant study

The antioxidant activity of green synthesized AgNPs was carried out according to the standard method [29] with some modifications. Different concentrations of synthesized AgNPs and standard ascorbic acid (10 μg/mL, 20 μg/mL, 40 μg/mL, 80 μg/mL, 160 μg/mL and 320 μg/mL) were prepared separately in a test tube from 50 mg/mL stock solution and 3 mL of 0.1 mM methanolic solution. DPPH was added to each of the prepared solution and incubated in dark area for 20 min. After incubation, absorbance of the solutions was measured using double beam UV-Vis spectrophotometer at 517 nm against methanol as blank. The methanolic solution DPPH without sample was used as control and the antioxidant activity in terms of percentage inhibition was calculated by the following formula (Equation 1).

$$\text{Percentage inhibition (\%)} = [(\text{Control Abs} - \text{Sample Abs})/(\text{Control Abs})] \times 100 \quad \text{Eq. 1}$$

Where,

Abs = Absorbance

3. Results and discussion

3.1. Phytochemical analysis of the plant leaf extracts

Qualitative phytochemical screening analysis was done on HAPLE to determine the presence of some phytochemicals in the leaves of this medicinal plant. The presence and/or absence of useful bioactive compounds such as alkaloids, tannins, flavonoids, terpenoids, phenols, saponins and anthraquinones in leaf extracts were revealed by the confirmatory test, involving color changes, precipitate formation and other confirmations. The phytochemical characteristics of the HAPLE are summarized in Figure 2 and Table 2 below. The results revealed that bioactive compounds like phenols, tannins, flavonoids, Alkaloids, anthraquinone, and saponins are present in the leaf of *Hagenia abyssinica*, while terpenoids and steroids were absent in this plant leaf. The presence of these bioactive components may play a major role in the reducing, capping and stabilization of AgNPs [15].

3.2. AgNPs biosynthesis

The AgNPs were successfully synthesized using 1:2 volume ratio of $AgNO_3$ to HAPLE as a reducing and capping agent, silver nitrate as a precursor and with other optimized parameters. It was observed that the colorless silver nitrate solution turned dark-brown on addition of leaves extract, while no color change was observed in the absence of plant extract (Figure 3). This change in color of the reaction mixture was taken as a primary evidence for the formation of AgNPs [31]. The synthesized AgNPs (Figure 3 f, g) were later subjected to various characterization methods.

Phytochemicals/secondary metabolites in plants are regarded as reducing agents in the green synthesis. Despite the complete vision of metal nanoparticles synthesis by using plants is not well understood until now, the phytochemicals of the plants led to the production of metal nanoparticles. Oxygen produced from degrading phytochemicals links the reduced metal ions. They are stabilized by phytochemicals that prevent agglomeration between them. For instance, Figure 4: saponins present in the plant extract interact with the Ag^+ ions through the hydroxyl groups present in saponins, leading to the formation of AgNPs, also providing stability for the newly formed nanoparticles. Flavonoids interact with the metallic ions via carbonyl functional groups present in the extract, liberating the reactive hydrogen, which then converts the enol in the flavonoid to keto form leading to the Ag^0 formation. Some proposed bio-reduction mechanism for AgNPs by phytochemicals are illustrated in (Figures 4, 5, and 6) [32].

3.3. Characterization of synthesized silver nanoparticles

3.3.1. UV-Visible spectroscopy analysis

Monitoring the process of the bio reduction of silver ions to AgNPs was applied in this study by UV-Vis spectroscopy. UV-Vis spectroscopy might be used to detect the size and shapeof the NPs in aqueous suspensions. The formation and optimization of AgNPs were monitored using UV–Vis spectroscopy by measuring the absorbance in the scanning range of 200–800 nm. The change in color indicates the formation of AgNPs which was further confirmed by the appearance of characteristic Surface Plasmon Resonance (SPR) peak between 400 to 500 nm [33]. The synthesized AgNPs were dark-brown in aqueous solution due to excitation of electrons and changes in electronic energy levels, reflecting the reduction of Ag^+ into Ag^0 [34]. Formation of silver nanoparticles was confirmed by the observed peaks in the range of 400–430 nm (Figures 7a-e). The different

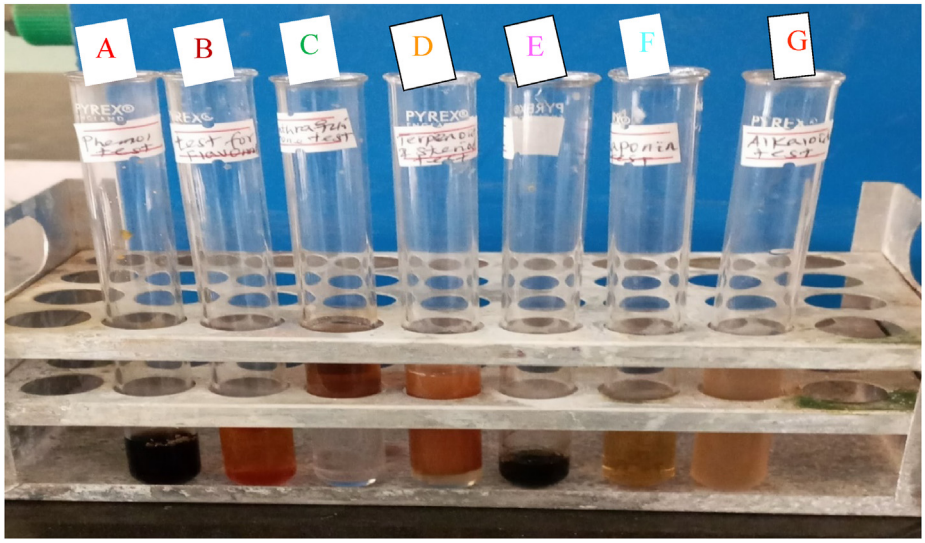

Figure 2. The color change observed when the leaf extract of *Hagenia abyssinica* was tested for the presence and absence of (A) Phenols, (B) Flavonoids, (C) Anthraquinones, (D) Terpenoids and steroids, (E) Tannins (F) Saponins and (G) Alkaloids.

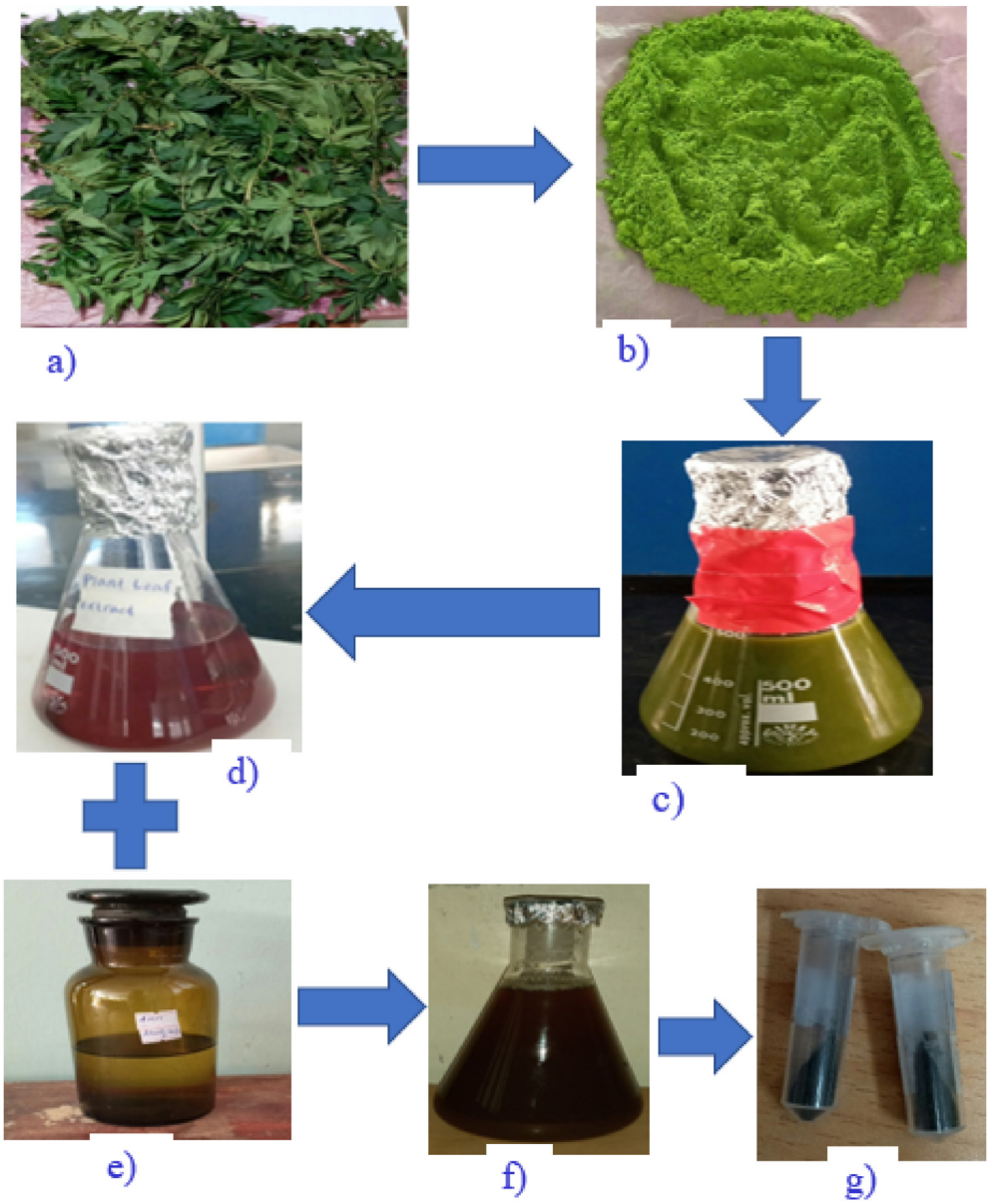

Figure 3. Green synthesis of AgNPs from HAPLE after incubation at 40 °C for 90 min, and colour change observation: a) *Hagenia abyssinica* plant leaf; b) *Hagenia abyssinica* plant leaf powder; c) Macerated *Hagenia abyssinica* aqueous plant leaf extract before filtration; d) *Hagenia abyssinica* aqueous plant leaf extract after filtration (dark-red); e) 4 mM aqueous $AgNO_3$ solution; (colorless); f) Colloidal AgNPs (dark-brown) and g) Powdered AgNPs.

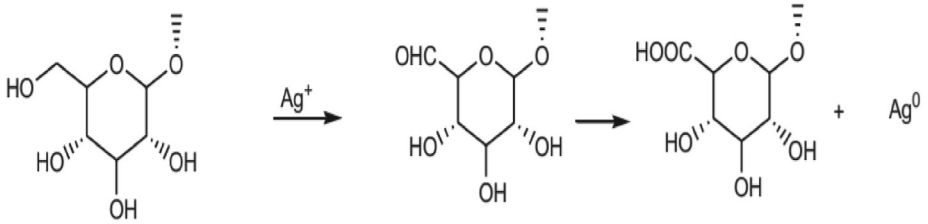

Figure 4. Phyto-reduction of Ag^+ to AgNPs by saponins.

parameters like temperature, pH, time, silver nitrate concentration and volume of leaf extract affect the synthesis of AgNPs.

3.3.2. Effects of operational parameters for the synthesis of AgNPs

The synthesis of AgNPs depends largely on some operational parameters. These parameters influence the nanoparticles synthesis irrespective of the technique used. In this study, evaluation of several important experimental factors, including reaction time (10 min, 30 min, 60 min, 90 min and 120 min); temperature (25 °C, 40 °C, 60 °C and 80 °C); concentration of silver ion solution (0.5 mM, 1 mM, 2 mM, 4 mM, and 6 mM); volume ratio of 1:1, 1:2, 1:3, 1:4, (silver ion solution to HAPLE); and pH of the reaction mixture (pH 4, pH 6, pH 7, pH 8, and pH

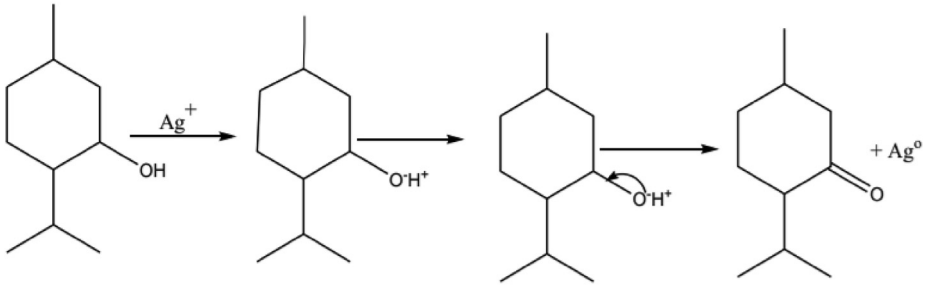

Figure 5. Phyto-reduction of Ag^{+} to AgNPs by terpenoids.

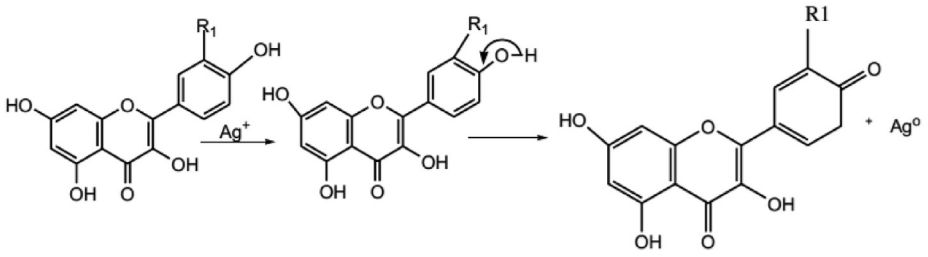

Figure 6. Phyto-reduction of Ag^{+} to AgNPs by flavonoids.

9) were studied. Each of these experimental factors was monitored by UV–Vis spectrophotometer.

3.3.2.1. Effects of silver ion concentration on the synthesis of AgNPs. The effect of concentration on the synthesis of AgNPs from HAPLE and $AgNO_3$ was shown in the UV-Vis spectra (Figure 7a). This operational parameter was monitored at various concentrations of silver ion solution. The experiment was carried out on the following series of silver ion concentration: 0.5 mM, 1 mM, 2 mM, 4 mM, and 6 mM. For the different concentrations, the intensity was increased with an increase in the concentration of Ag^{+} ion. A distinctive SPR peak and maximum absorbance was observed at a wavelength of 406 nm for a concentration of 4 mM $AgNO_3$ solution and this was considered as an optimal value for the synthesis of AgNPs. The height of the absorption peak of UV-Vis spectrum around 406 nm intensifies as the concentration of silver nitrate increased. The maximum peak intensity was obtained at 4 mM of $AgNO_3$ (Figure 7a). Peaks of different heights at 406 nm confirm the production of AgNPs with no change in wavelength. Varying the concentration of Ag^{+} ion solution affects the size and shape of the AgNPs produced and this result correlates with [35]. Results of [36] showed that 6 mM concentration of silver nitrate using *Aegle marmelos* leaf extracts as a reducing agent gave the maximum formation with the absorbance peak at 400–420 nm and the color turned to brown. The absorption peaks of AgNPs synthesized from leaf extract of *Clinacanthus nutans* were found between 442 nm–455 nm. The highest concentration of $AgNO_3$ yielded the highest absorption with slightly lower wavelength which indicates the highest amount of AgNPs being synthesized. Based on the absorption spectrum, the highest formation of AgNPs was observed at 5 mM concentration of $AgNO_3$ in [37].

The rate of formation of AgNPs was found to be slower at lower $AgNO_3$ concentration and hence causing weaker absorbance. In this study, a single SPR band was observed for each concentration of $AgNO_3$ and revealing spherical shape of silver nanoparticles. Spherical nanoparticles, disks, and triangular nanoplates of silver show one, two, and more SPR peaks, respectively [38].

3.3.2.2. Effects of volume ratio of $AgNO_3$ to plant leaf extract. Following the procedure in [39], effects of volume ratio was studied by varying the volume ratio of 4 mM Ag^{+} solution to the leaf extract in the ratio 1:1, 1:2, 1:3, and 1:4 by keeping constant volume of $AgNO_3$ solution. The absorption peak at 406 nm with maximum absorbance was recorded at 1:2 volume ratio (5 mL $AgNO_3$ solution to 10 mL HAPLE) and it was an optimized condition for the synthesis of AgNPs. The absorption peaks were slightly broader and lower absorbance was recorded for 1:1, 1:3 and 1:4 volume ratios with lower and higher volume of extract which indicates a slow reduction of Ag^{+} to Ag^{0} as shown in Figure 7b. Thus, other optimization parameters were carried out using this optimum volume ratio. It was in a good agreement with the previously studied and synthesized AgNPs from *Ocimum gratissmum* aqueous leaf extract by [39].

3.3.2.3. Effects of temperature for the synthesis of AgNPs. Figure 7c showed the UV–Vis absorption spectra of AgNPs obtained from aqueous solution of $AgNO_3$ with HAPLE. The spectra were recorded at 25 °C, 40 °C, 60 °C and 80 °C by keeping other optimal conditions constant. With all the different temperatures used, the color of the silver nanoparticles changed from light yellow to dark-brown. It was observed that maximum absorption has been recorded at 40 °C with maximum wave length of 402 nm and the absorption intensity was slightly increased in comparison with the others. This shows that at lower temperatures the plasmon peak showed a bathochromic shift at 60 °C and 80 °C. This bathochromic shift indicated that the mean diameter of the silver nanoparticles decreased [40]. The formation of silver nanoparticles at 40 °C indicated the ability of HAPLE to reduce silver ion and stabilize it without employing high temperature.

Therefore, the best condition for synthesis of AgNPs using HAPLE was taken at 40 °C based on the UV-Visible spectra of maximum absorption and amount of AgNPs produced. This was in good agreement with the previous reports in [41, 42]. Further optimization of other operational parameters was carried out at 40 °C which was the optimum temperature obtained.

3.3.2.4. Effects of reaction time for the synthesis of AgNPs. The effect of reaction time was studied by monitoring the reaction of the aqueous plant extract and $AgNO_3$ solution for 10 min, 30 min, 60 min, 90 min, and 120 min at 40 °C. At the moment HAPLE reacts with the solution of $AgNO_3$, a color change was observed from colorless to brown within 10 min of reaction. The color intensified with increase in time. The

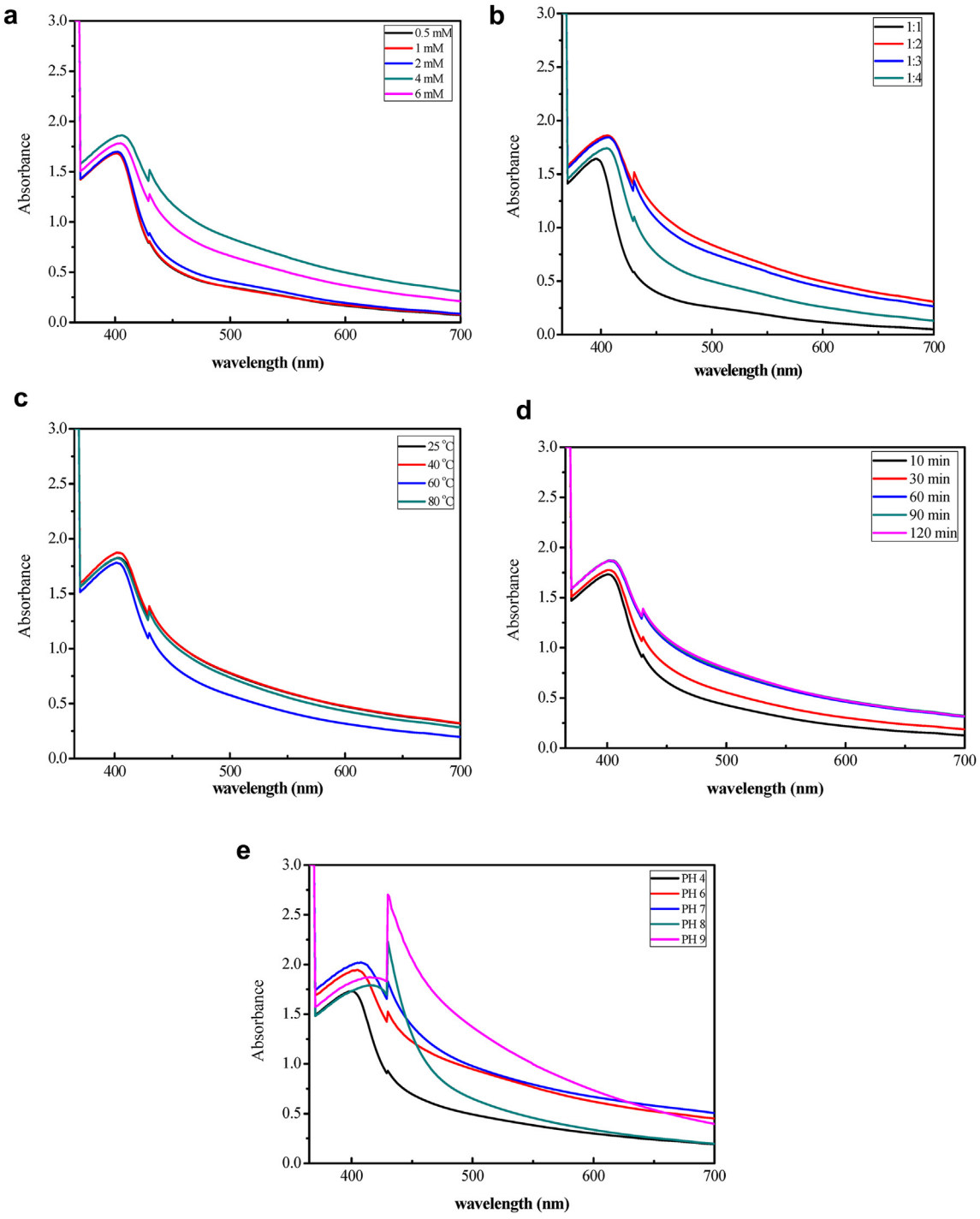

Figure 7. (a)UV–Vis absorption spectra of AgNPs synthesized by HAPLE at different $AgNO_3$ concentration. (b) UV-Vis absorption spectra of AgNPs synthesized by varying volume ratio of $AgNO_3$ solution to HAPLE by keeping constant the concentration & volume of $AgNO_3$ solution. (c) UV-Vis absorption spectra of temperature optimization for the synthesis of AgNPs from HAPLE. (d) UV-Vis absorption spectra of reaction time optimization for the synthesis of AgNPs from HAPLE. (e) UV-Vis spectra of pH optimization for the green synthesis of AgNPs from HAPLE.

UV–Visible measurements were recorded at various time intervals as shown in Figure 7d. It can be suggested that between zero and 10 min, the SPR band is slightly broadened because of the slow conversion of silver ion (Ag^+) to zerovalent silver (Ag^0) nanoparticles. Excellent SPR band and maximum absorption was observed as the reaction time increases because large amount of Ag^+ has been converted to Ag^0. The measured UV–Vis absorption spectra of the synthesized AgNPs showed best SPR peak within 402 nm at 90 min reaction time and this was agreed with the previous study reported by [28].

3.3.2.5. Effects of pH for the synthesis of AgNPs. The pH of green synthesized AgNPs without any pH optimization was adjusted using 1 M HCl and 1 M NaOH to a final pH of pH 4, pH 6, pH 7, pH 8, and pH 9 and their absorbance was measured by double beam UV-Vis spectrophotometer in

the scanning range of 200 nm–800 nm as depicted in Figure 7e. The SPR peaks for acidic conditions (pH 4 and pH 6) and neutral condition (pH 7) appear at a relatively short wavelength of around 405 nm while the SPR peaks are shifted towards a longer wavelength at ~430 nm in the basic medium (pH 8 and pH 9). The longer wavelength shift in a basic medium indicates relatively large AgNPs sizes compared with neutral and acidic conditions. Moreover, the intensity of SPR peaks tends to increase when the pH value increases whereas the intensity of SPR peaks for acidic conditions decreases with increasing pH [43].

Enhanced synthesis of AgNPs under alkaline conditions may be due to more availability of bio-reductants. This could be attributed to changes in the dissociation constant values of the functional groups present in the biomolecules involved in the reduction of Ag^{+} ions. Furthermore, the decreased reduction rate in acidic medium could be ascribed to the denaturation and/or degradation of bioactive compounds present in the plant leaf extract [39].

3.3.3. FT-IR analysis

To check the capped biomolecules with AgNPs, FTIR study was performed to confirm the functional groups (which is responsible for reduction, stabilization and capping agents) and it was compared with the FTIR spectrum of leaves extract alone. FT-IR absorption spectra of green synthesized AgNPs and HAPLE was studied in the range of 400 cm^{-1}-4000 cm^{-1} as presented in Figure 8.

The FTIR analysis was done for both plant leaf extract and green synthesized AgNPs. Figure 8(a) revealed the FT-IR spectrum of HAPLE. A broad band around 3412.52 cm^{-1} is due to the N–H stretching vibration of NH_2 group and O–H group of the overlapping of the stretching vibration attributed to water and phenolic compounds present in HAPLE. The peak at 2933.62 cm^{-1} corresponds to C–H stretching modes. The stretching mode of carbonyl group (C=O) was observed at 1614.92 cm^{-1}, suggesting the presence of carboxylic, aldehydes, esters or ketone containing compounds arising from flavonoids and tannins. The bands at ~1402.77 cm^{-1} were assigned for N–H stretching vibration present in the amide linkages. The intense band at 1041.87 cm^{-1} could be assigned to the C–N stretching vibrations of aliphatic amines and bands at 1190.63 cm^{-1} is due to the C–O group of aliphatic esters. The green synthesized AgNPs showed the major and strongest vibrational modes at around 752 cm^{-1}, 1049.41 cm^{-1}, 1183.09 cm^{-1}, 1363.23 cm^{-1}, 1646.30 cm^{-1}, 2925.46 cm^{-1}, and 3396.19 cm^{-1} as located in Figure 8(b). A broad peak around 3396.19 cm^{-1} corresponds to –OH stretching of phenolic compounds and N–H stretching vibrations of amino groups present in the plant leaf extract. The peak at 2925.46 cm^{-1} corresponds to C–H stretching modes and the peak at 1646.30 cm^{-1} corresponds to C=O stretching and N–H bending primary amides.

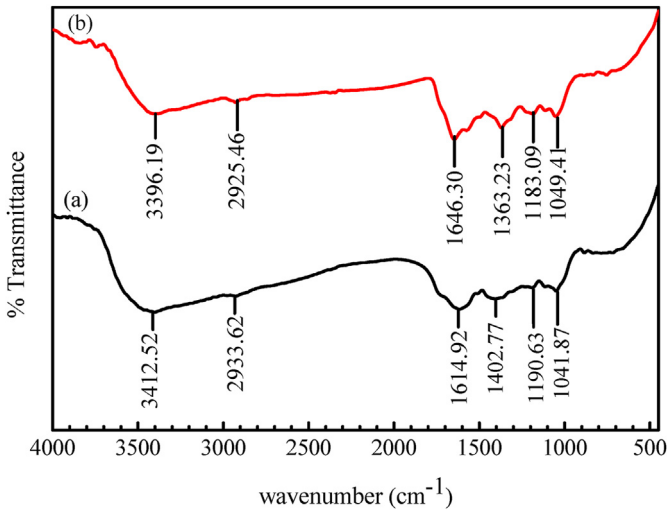

Figure 8. FTIR spectra of (a) HAPLE and (b) Synthesized AgNPs.

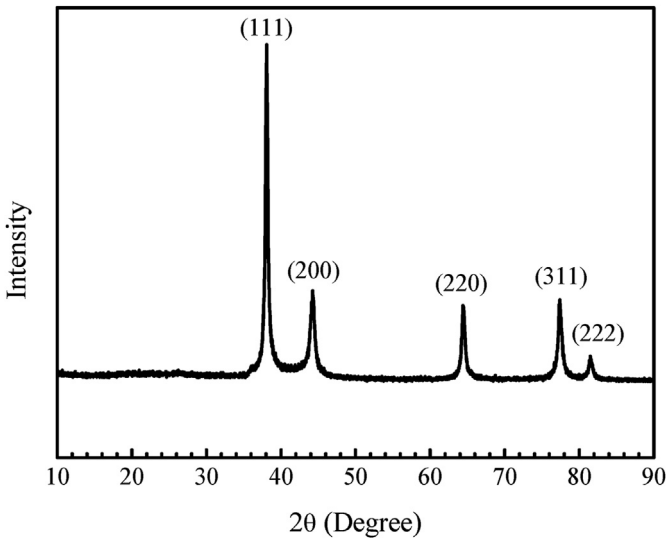

Figure 9. XRD pattern of green synthesized AgNPs from HAPLE.

An intense peak around 1363.23 cm^{-1} shows N–H stretch vibration in the amide linkage and bands at 1183.09 cm^{-1} is due to the C–O group of aliphatic esters. The intense band at 1049.41 cm^{-1} could be assigned to the C–N stretching vibrations of aliphatic amines. All the observed FT-IR spectra analysis was comparable with previous studies [40, 44, 45]. The FTIR band of synthesized AgNPs in Figure 8(b) showed a little change in position and intensity in the peaks. The displacement at 3396.19 cm^{-1} may be related to hydrogen bond breakage, which plays a role in reducing silver ions into silver nanoparticles. The similarity of spectral pattern for plant leaf extract and the synthesized nanoparticles may be an evidence for the existence of the identified phytochemicals in the synthesized AgNPs [46].

3.3.4. XRD pattern analysis

Figure 9 shows an XRD pattern for the prepared AgNPs using HAPLE. The XRD analysis was performed to evaluate the crystalline structure, size, and purity of the prepared AgNPs. In the XRD pattern, five prominent diffraction peaks were observed at $2\theta = 38.08°$, 44.29°, 64.43°, 77.30°, and 81.58° which could be attributed to (111), (200), (220), (311), and (222) diffraction planes, respectively. All the diffraction peaks were attributed from the cubic structure of pure Bragg's reflections of the face-centered cubic (FCC) structure of metallic silver powder phase [47]. These planes confirmed the crystalline nature of the green synthesized AgNPs. The highest peak intensity of (111) plane with narrow full width at half maximum (FWHM) illustrates the good crystalline nature of synthesized AgNPs as observed from the XRD patterns. The resulted peaks and their corresponding Bragg's reflections are strongly agreed with the Joint Committee on Powder Diffraction Standards (JCPDS, file no. 04–0783). The prominent characteristic peaks of the green synthesized silver nanoparticles indicate the purity of the synthesized nanoparticles without any additional diffraction peaks. The average crystallite sizes of the particles were calculated by using Debye-Scherrer's equation (Equation 2):

$$D = \frac{K\lambda}{\beta \cos\theta} \qquad \text{Eq. 2}$$

where, D is the estimated crystal size in nanometere (nm) from XRD patterns, θ is the Bragg angle in radians, λ is the wavelength of X-ray source used (CuK_{α} = 1.5406 Å), β is the angular width at the half maximum of the diffraction peak in radians and K is the shape factor or Scherrer constant (0.9) of Debye-Scherrer's equation. The estimated average crystalline size (D) of the synthesized silver nanoparticles is found to be 22.2 nm.

3.4. Anti-bacterial studies of green synthesized AgNPs

Biosynthesized AgNPs from HAPLE and the leaf extract alone as a comparison were studied for their antibacterial activity against clinically isolated two Gram-negative bacteria *(klebsiella pneumoniae* and *salmonella typhimurium)* and one Gram-positive bacteria (*Streptococcus pneumoniae*) by following standard agar well diffusion method, and Zone of Inhibition (ZOI) was recorded.

Antibacterial activity was shown by ZOI which was characterized by a clear zone between the wells (containing samples) and a certain distance. Formation of ZOI around the wells showed bacterial sensitivity to antibacterial and antibiotic drugs (which are used as a positive controls). The positive control used in the well was a ciprofloxacin and functioned as a control of the test solution by comparing the diameter of the ZOI formed. On the contrary, DMSO as a negative control was used to determine the effect of solvents in the test solution on the growth bacteria. The ZOI on all bacterial strains was measured after 24 h of incubation time at 37 °C.

As clearly described by Figure 10 and Table 3, the synthesized AgNPs and plant leaf extract showed anti-bacterial activity against all bacterial strains tested. However, it was more effective against gram-negative (*salmonella typhimurium*) bacteria in both the synthesized nanoparticle and the plant crude extract. As the concentration of the synthesized AgNPs and plant leaf extract increases the anti-bacterial activity also increased. The anti-bacterial activity of green synthesized AgNPs against gram-negative (*salmonella typhimurium*) bacteria was maximum with ZOI of 18.3 mm with respect to the highest concentration (200 μg/mL) (Table 3). Whereas the anti-bacterial activity of the plant leaf extract alone against gram-negative (*salmonella typhimurium*) bacteria in terms of maximum ZOI (13 mm) was recorded with the highest concentration of 200 μg/mL (Table 3). Based on this result, one can conclude that the green synthesized AgNPs had highest anti-bacterial activity against gram-negative bacteria strains specially *salmonella typhimurium* as compared to the plant leaf extract. The studies of this result correlate with the previous report [29].

The highest anti-bacterial activity of green synthesized AgNPs against gram-negative bacteria (*salmonella typhimurium*) was probably due to large surface area of the nanoparticles which provide better contact with the microorganisms and will have stronger bactericidal effect than larger particles. This anti-bacterial difference can also be due to the difference in the composition of their cell wall, as the cell membrane of gram-negative bacteria consists of a single layer of peptidoglycan, while multiple layers of peptidoglycan are present in the membrane of gram-positive bacteria, which makes them more rigid. The silver ions from nanoparticles are attracted by the negative charge of the bacterial cell wall, and when they experience some electrostatic attraction toward the bacterial cell wall, they will move and get attached to the cell wall and lead to a change in the composition of the cell wall by affecting its permeability [15].

3.5. Anti-oxidant studies of green synthesized AgNPs

The antioxidant activity of the synthesized AgNPs was determined by using DPPH free radical assay and ascorbic acid as a reference standard. The synthesized AgNPs and standard ascorbic acid was separately prepared in a test tube with different concentrations (10–320 μg/mL) from 50 mg/mL stock solution and absorbance of each sample was measured using UV-Visible spectrophotometer. The methanolic solution of DPPH without sample was used as control. The results obtained are summarized in Table 4 and Figure 11.

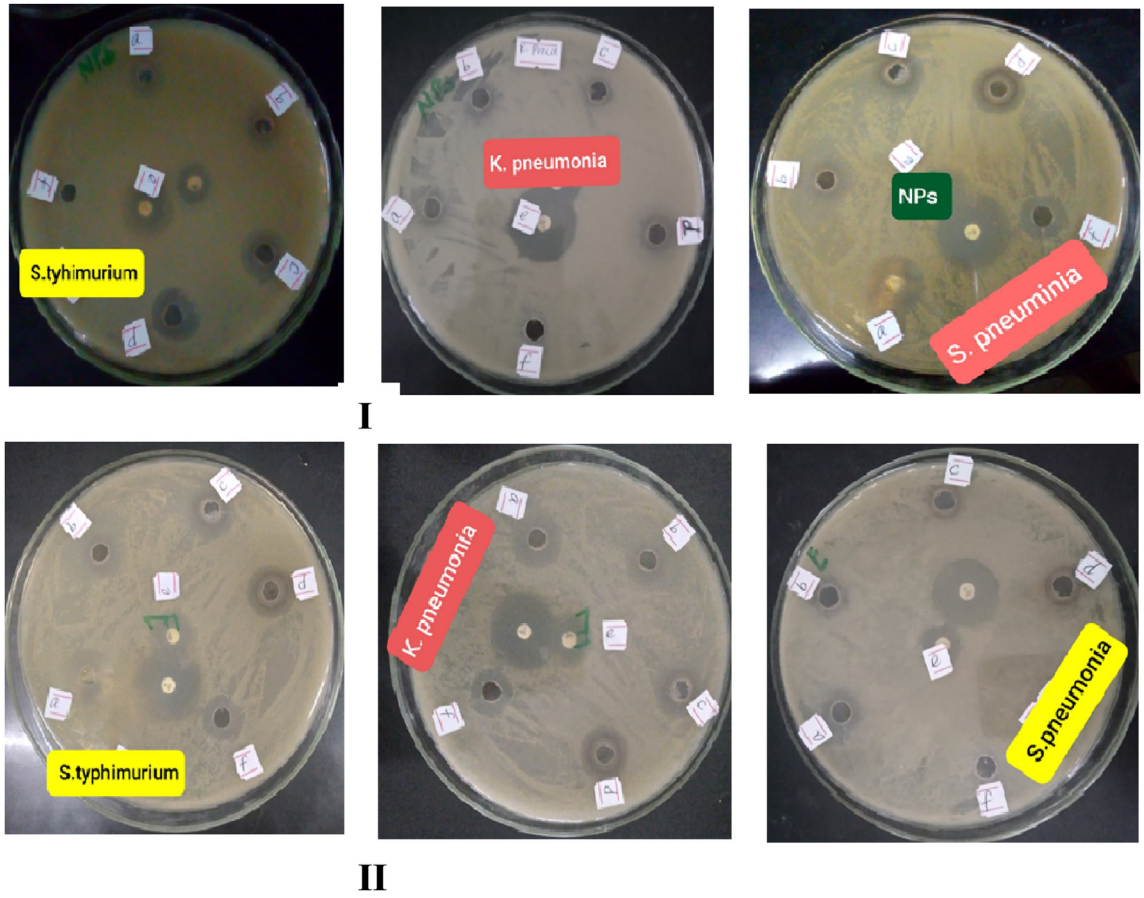

Figure 10. **(I)** Antibacterial activity of synthesized AgNPs and **(II)** HAPLE alone; (a = 50 μg/mL, b = 100 μg/mL, c = 150 μg/mL, d = 200 μg/mL, e = ciprofloxacin (positive control), and f = DMSO (negative control)).

Table 3. Antibacterial activity of green synthesized AgNPs and HAPLE against clinically isolated human pathogenic bacteria.

Concentration (μg/ml)	AgNPs			HAPLE		
	Mean diameter of ZOI (in mm) for the tested bacteria			Mean diameter of ZOI (in mm) for the tested bacteria		
	S. typhi	*K. pneumoniae*	*S. pneumoniae*	*S. typhi*	*K. pneumoniae*	*S. pneumoniae*
50	14	10	6.4	7	5	3
100	16.3	10.6	7	9.6	7.3	4
150	17.3	12	7.3	10	9	4.6
200	18.3	14	8.6	13	10	6.3
Cipro	20	21	19	23.3	24	18
DMSO	0	0	0	0	0	0

Ciprofloxacin = Cipro.
klebsiella pneumoniae = *K. pneumoniae*; *salmonella typhimurium* = *S. typhi*.
Streptococcus pneumoniae = *S. pneumoniae*.

Table 4. Antioxidant activity of green synthesized AgNPs and ascorbic acid (standard) in terms of percentage inhibition DPPH radical scavenging activity.

Concentration of AgNPs (μg/mL)	% Inhibition (DPPH Radical Scavenging Activity)
10	30.6
20	35.2
40	39.4
80	48.6
160	60.6
320	66.0
Concentration of standard ascorbic acid (μg/mL)	**% Inhibition (DPPH Radical Scavenging Activity)**
10	57.7
20	63.0
40	77.0
80	87.2
160	92.7
320	95.9

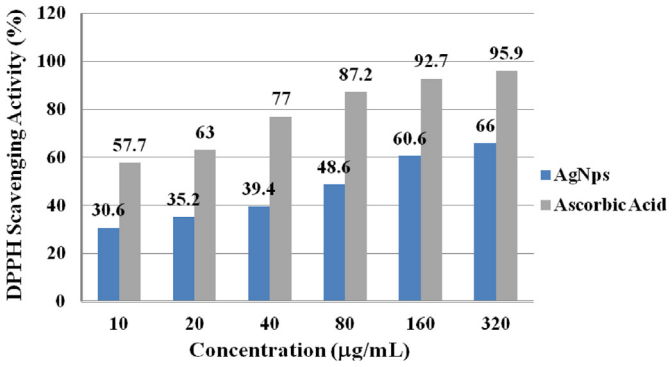

Figure 11. DPPH radical scavenging activity of synthesized AgNPs from HAPLE.

As clearly described in Figure 11, the anti-oxidant properties of green synthesized AgNPs increased with increasing concentration in the range 10 μg/mL-320 μg/mL, thereby increasing the DPPH radical scavenging ability. A dose-dependent pattern was observed in the scavenging activity, which increased with increase in dose of AgNPs. The scavenging potential of the green synthesized AgNPs was comparatively lower than that of standard ascorbic acid.

A concentration of 320 μg/mL (maximum tested concentration) for green synthesized AgNPs exhibited the highest anti-oxidant activity (inhibition concentration of 66%) and lower than that of the standard ascorbic acid (95.9%) with similar tested concentration. Similar observations with increased DPPH scavenging activity of AgNPs synthesized from *Elephantopus scaber* leaf extract have been reported [48]. The finding of the present study reveals that the synthesized AgNPs possessed anti-oxidant property in terms of free radical scavenging activity.

By the same procedure, the antioxidant activity of the *Hagenia abyssinica* plant leaf extract was tested using DPPH free radical assay and ascorbic acid as a reference standard. Compared to AgNPs, the *Hagenia abyssinica* plant leaf extract possessed a little anti-oxidant property in terms of free radical scavenging activity.

4. Conclusion

AgNPs were successfully synthesized from *Hagenia abyssinica* plant leaf extract as a reducing and capping agents. The synthesized AgNPs were fully characterized by UV-Visible spectroscopy, FTIR and XRD. The presence of bioactive-molecules (phenols, tannins, flavonoids, alkaloids, anthraquinones, and saponins) present in the plant leaf extract observed from phytochemical screening was confirmed by FT-IR. Surface plasmon resonance with intense peak was observed at 430 nm by UV-Vis spectrophotometric measurements with the optimized values. The crystalline structure with FCC geometry and with the average crystallite size of 22.2 nm was determined by XRD analysis. The synthesized AgNPs and the plant leaf extract exhibited significant antibacterial activity against both gram-negative (*Klebsiella pneumonia* and *Salmonella typhimurium*) and gram-positive bacteria (*Streptococcus pneumonia*). But, the synthesized AgNPs showed strong inhibition in gram-negative bacteria compared to the same tested pathogenic bacteria strain of the plant leaf extract. From the results of DPPH free radical scavenging assay, the green synthesized AgNPs showed anti-oxidant property in the tested concentrations. From this study, it can be inferred that the synthesized AgNPs could be used in the fields of water treatment, biomedicine, biosensor and nanotechnology.

Declarations

Author contribution statement

Walelign Wubet Melkamu: conceived and designed the experiments; analyzed and interpreted the data; contributed reagents, materials, analysis tools or data; wrote the paper.

Legesse Terefe Bitew: conceived and designed the experiments; performed the experiments; analyzed and interpreted the data; contributed reagents, materials, analysis tools or data.

Funding statement

This research did not receive any specific grant from funding agencies in the public, commercial, or not-for-profit sectors.

Data availability statement

Data will be made available on request.

Declaration interest statement

The authors declare no conflict of interest.

Additional information

No additional information is available for this paper.

References

[1] R. Arif, R. Uddin, A review on recent developments in the biosynthesis of silver nanoparticles and its biomedical applications, Med Devices Sens 4 (2020) 1–20.

[2] H.M. Tag, A.A. Saddiq, M. Alkinani, N. Hagagy, Biosynthesis of silver nanoparticles using *Haloferax* sp. NRS1: image analysis, characterization, in vitro thrombolysis and cytotoxicity, Amb. Express 11 (2021) 1–12.

[3] W.A. Lotfy, B.M. Alkersh, S.A. Sabry, H.A. Ghozlan, Biosynthesis of silver nanoparticles by Aspergillus terreus: characterization, optimization, and biological activities, Front. Bioeng. Biotech. 9 (2021) 1–14.

[4] K. Khan, S. Javed, Silver nanoparticles synthesized using leaf extract of Azadirachta indica exhibit enhanced antimicrobial efficacy than the chemically synthesized nanoparticles: a comparative study, Sci. Prog. 104 (2021) 1–15.

[5] Y.K. Mohanta, S.K. Panda, A.K. Bastia, T.K. Mohanta, Biosynthesis of silver nanoparticles from protium serratum and investigation of their potential impacts on food safety and control, Front. Microbiol. 8 (2017) 1–10.

[6] Md.M.I. Masum, Mst.M. Siddiqa, K.A. Ali, Y. Zhang, Y. Abdallah, E. Ibrahim, W. Qiu, C. Yan, B. Li, Biogenic synthesis of silver nanoparticles using Phyllanthus emblica fruit extract and its inhibitory action against the pathogen acidovorax oryzae strain RS-2 of rice bacterial Brown stripe, Front. Microbiol. 10 (2019) 1–18.

[7] C. Vanlalveni, S. Lallianrawna, A. Biswas, M. Selvaraj, B. Changmai, S.L. Rokhum, Green synthesis of silver nanoparticles using plant extracts and their antimicrobial activities: a review of recent literature, RSC Adv. 11 (2021) 2804–2837.

[8] S. Jain, M.S. Mehata, Medicinal plant leaf extract and pure flavonoid mediated green synthesis of silver nanoparticles and their enhanced antibacterial property, Sci. Rep. 7 (2017) 1–13.

[9] M. Shah, D. Fawcett, S. Sharma, S.K. Tripathy, G.E.J. Poinern, Green synthesis of metallic nanoparticles via biological entities, Materials 8 (2015) 7278–7308.

[10] S. Pirtarighat, M. Ghannadnia, S. Baghshahi, Green synthesis of silver nanoparticles using the plant extract of *Salvia spinosa* grown in vitro and their antibacterial activity assessment, J. Nanostruc. Chem. 9 (2019) 1–9.

[11] A. Salayová, Z. Bedlovicová, N. Daneu, M. Baláž, Z.L. Buj ňáková, L. Balážová, L. Tkáčiková, Green synthesis of silver nanoparticles with antibacterial activity using various medicinal plant extracts: morphology and antibacterial efficacy, Nanomaterials 11 (2021) 1–20.

[12] J. Balavijayalakshmi, V. Ramalakshmi, Carica papaya peel mediated synthesis of silver nanoparticles and itsantibacterial activity against human pathogens, J. Appl. Res. Technol. xx (2017) 1–10.

[13] E.K. Kambale, C.I. Nkanga, B.-P.I. Mutonkole, A.M. Bapolisi, D.O. Tassa, J.-M.I. Liesse, R.W.M. Krause, P.B. Memvanga, Green synthesis of antimicrobial silver nanoparticles using aqueous leaf extracts from three Congolese plant species (Brillantaisia patula, Crossopteryx febrifuga and Senna siamea), Heliyon 6 (2020), e04493.

[14] S. Veeramani, E. Ravindran, P. Ramadoss, C. Joseph, K. Shanmugam, S. Renganathan, Silver nanoparticles - green synthesis with aq. Extract of stems *Ipomoea pes-caprae*, characterization, antimicrobial and anti-cancer potential, Int J Med Nano Res 5 (2018) 1–9.

[15] Hemlata, P.R. Meena, A.P. Singh, K.K. Tejavath, Biosynthesis of silver nanoparticles using cucumis prophetarum aqueous leaf extract and their antibacterial and antiproliferative activity against cancer cell lines, ACS Omega 5 (2020) 5520–5528.

[16] M.J. Firdhouse, P. Lalitha, Biosynthesis of silver nanoparticles and its applications, J. Nanotechn. 2015 (2015) 1–19.

[17] S. Liao, Y. Zhang, X. Pan, F. Zhu, C. Jiang, Q. Liu, Z. Cheng, G. Dai, G. Wu, L. Wang, L. Chen, Antibacterial activity and mechanism of silver nanoparticles against multidrug-resistant *Pseudomonas aeruginosa*, Int. J. Nanomed. 14 (2019) 1469–1487.

[18] Z. Breijyeh, B. Jubeh, R. Karaman, Resistance of gram-negative bacteria to current antibacterial agents and approaches to resolve it, Molecules 25 (2020) 1–23.

[19] U. Nagaich, N. Gulati, S. Chauhan, Antioxidant and antibacterial potential of silver nanoparticles: biogenic synthesis utilizing apple extract, J. Pharm. 2016 (2016) 1–8.

[20] A.O. Akintola, B.D. Kehinde, P.B. Ayoola, A.G. Adewoyin, O.T. Adedosu, J.F. Ajayi, S.B. Ogunsona, Antioxidant properties of silver nanoparticles biosynthesized from methanolic leaf extract of *Blighia sapida*, IOP Conf. Ser. Mater. Sci. Eng. 805 (2020) 1–18.

[21] B. Assefa, G. Glatzel, C. Buchmann, Ethnomedicinal uses of *Hagenia abyssinica (Bruce) J.F. Gmel.* among rural communities of Ethiopia, J. Ethnobiol. Ethnomed. 6 (2010) 1–10.

[22] H.A. Murthy, T.D. Zeleke, C.R. Ravikumar, M.R.A. Kumar, H.P. Nagaswarupa, Electrochemical properties of biogenic silver nanoparticles synthesized using Hagenia abyssinica (Brace) JF. Gmel. medicinal plant leaf extract, Mater. Res. Express 7 (2020) 1–13.

[23] D. Kardong, S. Upadhyaya, L.R. Saikia, Screening of phytochemicals, antioxidant and antibacterial activity of crude extract of Pteridium aquilinum Kuhn, J. Pharm. Res. 6 (2013) 179–182.

[24] M. Kavit, B.N. Patel, B.K. Jain, Phytochemical analysis of leaf extract of Phyllanthus fraternus, Res. J. Rec. Sci. 2 (2013) 12–15.

[25] L.N. Madike, S. Takaidza, M. Pillay, Preliminary phytochemical screening of crude extracts from the leaves, stems, and roots of tulbaghia violacea, Int. J. Pharmacog. Phytochem. Res. 9 (2017) 1300–1308.

[26] R.P. Senthilkumar, V. Bhuvaneshwari, V. Malayaman, R. Ranjithkumar, S. Sathiyavimal, Phytochemical screening of aqueous leaf extract of *Sida acuta burm. F.* And its antibacterial activity, J. Emerg. Technolog. Innov. Res. 5 (2018) 474–478.

[27] S. Ahmed, M. Ahmad, B.L. Swami, Green synthesis of silver nanoparticles using Azadirachta indica aqueous leaf extract, J. Rad. Res. Appl. Sci. 9 (2015) 1–7.

[28] A.O. Dada, A.A. Inyinbor, O.M. Bello, A.P. Oluyori, T.A. Adelani-Akande, A.O. Abiodun, O. Dada, Effect of operational parameters, characterization and antibacterial studies of green synthesis of silver nanoparticles using Tithonia diversifolia, PeerJ 6 (2018) 1–17.

[29] A. Saravanakumar, M.M. Peng, M. Ganesh, M. Mohankumar, H.T. Jang, Low-cost and eco-friendly green synthesis of silver nanoparticles using *Prunus japonica* (Rosaceae) leaf extract and their antibacterial , antioxidant properties, Artif. Cells Nanomed. Biotechn. 1401 (2016) 1–8.

[30] G. Franci, A. Falanga, S. Galdiero, L. Palomba, M. Rai, G. Morelli, M. Galdiero, Silver nanoparticles as potential antibacterial agents, Molecules 20 (2015) 8856–8874.

[31] G.R.A. El-Chaghaby, A.F. Ahmad, Biosynthesis of silver nanoparticles using pistacia lentiscus leaves extract and investigation of their antimicrobial effect, Orient. J. Chem. 27 (2011) 929–936.

[32] S.O. Alayande, A.A. Akinsiku, O.B. Akinsipo, E.O. Ogunjinmi, E.O. Dare, Green synthesized silver nanoparticles and their therapeutic applications, Compr. Anal. Chem. xxx (2021) 1–27.

[33] H.M. Kredy, The effect of pH , Temperature on the green synthesis and biochemical activities of silver nanoparticles from Lawsonia inermis extract, J. Pharmaceut. Sci. Res. 10 (2018) 2022–2026.

[34] E.E. Elemike, D.C. Onwudiwe, O. Arijeh, H.U. Nwankwo, Plant-mediated biosynthesis of silver nanoparticles by leaf extracts of Lasienthra africanum and a study of the influence of kinetic parameters, Bull. Mater. Sci. 40 (2017) 129–137.

[35] M.M. Nadzir, F.N. Idris, K. Hat, Green synthesis of silver nanoparticle using Gynura procumbens aqueous extracts, AIP Conf. Proceed. 2124 (2019) 1–7.

[36] J.S.G. Christopher, B. Saswati, P.S. Ezilrani, Optimization of parameters for biosynthesis of silver nanoparticles using leaf extract of Aegle marmelos, Braz. Arch. Biol. Techn. 58 (2015) 702–710.

[37] S.N.A. Mat Yusuf, C.N.A. Che Mood, N.H. Ahmad, D. Sandai, C.K. Lee, V. Lim, Optimization of biogenic synthesis of silver nanoparticles from flavonoid-rich Clinacanthus nutans leaf and stem aqueous extracts, Royal Soci. Open Sci. 7 (2020) 1–15.

[38] A.A. Moosa, A.M. Ridha, M. Al-Kaser, Process parameters for green synthesis of silver nanoparticles using leaves extract of process parameters for green synthesis of silver nanoparticles using leaves extract, Int. J. Med. Clin. Res. 3 (2015) 966–975.

[39] K. Sharma, S. Guleria, V.K. Razdan, Green synthesis of silver nanoparticles using Ocimum gratissimum leaf extract: characterization, antimicrobial activity and toxicity analysis, J. Plant Biochem. Biotechnol. 29 (2020) 213–224.

[40] O.O. Oluwaniyi, H.I. Adegoke, E.T. Adesuji, A.B. Alabi, S.O. Bodede, A.H. Labulo, C.O. Oseghale, Biosynthesis of silver nanoparticles using aqueous leaf extract of Thevetia peruviana Juss and its antimicrobial activities, Appl. Nanosci. 6 (2016) 903–912.

[41] B. Ahmad, J. Ali, S. Bashir, Optimization and effects of different reaction conditions for the bioinspired synthesis of silver nanoparticles using *Hippophae r hamnoides linn* . Leaves aqueous extract, World Appl. Sci. J. 22 (2013) 836–843.

[42] L.R. Patil, A.R. Shet, A.G. Lohar, G.B. Tennalli, A. Sharanappa, V.S. Hombalimath, Optimization of process parameters for synthesis of silver nanoparticles using leaf extract of *tridax procumbent* and its biotechnological applications, Int. J. Scient. Techn. Res. 9 (2020) 1050–1056.

[43] P. Traiwatcharanon, K. Timsorn, C. Wongchoosuk, Flexible room-temperature resistive humidity sensor based on silver nanoparticles, Mater. Res. Express 4 (2017) 1–11.

[44] A.M. Awwad, N.M. Salem, A.O. Abdeen, Green synthesis of silver nanoparticles using carob leaf extract and its antibacterial activity, Int. J. Integrated Care 4 (2013) 1–6.

[45] V. Kumar, S. Singh, B. Srivastava, R. Bhadouria, Green synthesis of silver nanoparticles using leaf extract of *Holoptelea integrifolia* and preliminary investigation of its antioxidant, anti-inflammatory, antidiabetic and antibacterial activities, J. Environ. Chem. Engin. 7 (2019) 1–7.

[46] J.B.D. Sahar, D. Hoorieh, N. Farzaneh, H. Malak, Characterization and the evaluation of antimicrobial activities of silver nanoparticles biosynthesized from Carya illinoinensis leaf extract, Heliyon 6 (2020), e03624.

[47] M.M.H. Khalil, Green synthesis of silver nanoparticles using olive leaf extract and its antibacterial activity, Arab. J. Chem. 7 (2014) 1131–1139.

[48] S.N. Kharat, V.D. Mendhulkar, Synthesis , Characterization and studies on Antioxidant activity of Silver Nanoparticles using Elephantopus scaber leaf extract, Mater. Sci. Eng. C 62 (2016) 719–724.